J Appl Biol Chem (2014) 57(2), 113–122
http://dx.doi.org/10.3839/jabc.2014.017

Online ISSN 2234-7941
Print ISSN 1976-0442

Original Article: Biochemistry/Molecular Biology

A5E promotes Cell growth Arrest and Apoptosis in Non Small Cell Lung Cancer

Ye Sol Bak · Sun Young Ham · Baatartsogt O · Seung Hyun Jung · Kang Duk Choi · Tae Young Han · Il Young Han · Do-Young Yoon*

Received: 1 October 2013 / Accepted: 21 October 2013 / Published Online: 30 June 2014

Abstract A5E is complex of several medicinal herb ethanol extracts. The aim of this study is investigating the anticancer effect for non-small cell lung cancer. The antitumor effects of A5E on NCI-H460 were examined by regulation of cell proliferation, apoptosis, cell cycle arrest, mitochondrial membrane potential ($\Delta\psi_m$), and apoptosis-related protein. Cell proliferation was measured by MTS assay. Apoptosis induced by A5E was confirmed by Annexin V-fluorescein isothiocyanate (FITC)/Propidium Iodide (PI) staining, and cell cycle arrest was measured by PI staining. NF-κB translocation was detected by immunofluorescence and MMP ($\Delta\psi_m$) was measured by JC-1 staining. The expression of extrinsic pathway molecules such as FasL and FADD were elevated, and procaspase-8 was processed by A5E. In addition, intrinsic pathway related molecules were altered. The Bcl-2 and Bcl-xl levels decreased, Bax increased, and cytochrome C was released. In addition, the mitochondrial membrane potential collapsed, and caspase-3 and poly-(ADP-ribose) polymerase were processed by A5E. Moreover, A5E affected the cellular survival pathway involving phosphatidylinositol 3-kinase (PI3K)/Akt and NF-κB. PI3K and Akt were downregulated, also NF-κB expression was decreased, and nuclear translocalization was inhibited by A5E. These results suggested that A5E delays proliferation, inhibit cell cycle progression and induce apoptosis in human lung cancer cell. We conclude that_A5E is a potential anticancer agent for human lung carcinoma.

Keywords apoptosis · cell cycle · cytotoxicity · NCI-H460 · proliferation · traditional medicinal herb

Y. S. Bak · S. Y. Ham · D.-Y. Yoon
Department of Bioscience and Biotechnology, Bio/Molecular Informatics Center, Konkuk University, Seoul, Republic of Korea

B. O · S. H. Jung
School of Oriental Medicine, Dongguk University, Siksa dong, Ilsan, Republic of Korea

K. D. Choi
Graduate School of Bio & Information Technology, Hankyong National University, Ansung, Gyeonggi-do, Republic of Korea

T. Y. Han
Banryong Insu Herb Clinic, Nonhyun-dong, Gangnam-Gu, Seoul, Republic of Korea

I. Y. Han
Sunwun Biophysic, Ansung, Gyeonggi-do, Republic of Korea

*Corresponding author (D. Y. Yoon: ydy4218@konkuk.ac.kr)

Introduction

Lung cancer is a major cause of cancer deaths worldwide. Lung cancer is classified as non small cell lung cancer and small cell lung cancer (Massion and Carbone, 2003; Jemal et al., 2010). Usually, lung cancer cells have chromosomal abnormalities such as defects of the tumor suppressor genes p53 and Rb, which result in a failure to regulate apoptosis signals and cell proliferation (Massion and Carbone, 2003; Thafeni et al., 2012). In addition, lung cancer relapses easily, despite many therapies such as surgery, radiation, and chemotherapy (Mou et al., 2011). Therefore, development of alternative lung cancer agents is required. Several bioactive compounds from traditional Chinese medicinal herbs have been investigated (Hsu et al., 2008; Li et al., 2009). A5E is an ethanol extract of several herbs such as ginseng, chaga, pinellia, and tuber (Table 1), and several compounds in A5E are listed in Table 2. Each compound has been reported to possess anticancer effect in several cancers (Chung et al., 2010; Kim et al., 2010; Li et al., 2010). Some studies also revealed synergistic effects in Chinese medicine and herbs (Wang et al., 2008).

Apoptosis or programmed cell death is a highly regulated process involved in development and tissue homeostasis. Disruptions of apoptosis can lead to deleterious consequences as exemplified by several human disease states, including acquired immunodeficiency syndrome, neurodegenerative disorders, and cancer (Thompson. 1995; Kang et al., 2011). Apoptosis is controlled by pro-apoptotic caspases, proteases that are synthesized as inactive precursors, which are activated by proteolytic processing (Fischer et al., 2003). Two major pathways trigger apoptosis: a mitochondria-dependent pathway and a death-receptor pathway. The majority of chemotherapeutic agents trigger the mitochondrial pathway, but the death receptors have been reported to be involved in chemotherapy-induced apoptosis (Calviello et al., 2003). This article investigated the modulating effects of A5E on cell proliferation and apoptosis.

Table 1 The composition of A5E

Oriental Name	Country of origin	Grams	%
Ginseng	Korea	158	15.8
Chaga	Russia	158	15.8
Pinellia Tuber	China	106	10.6
Sparganium Rhizome	China	52	5.2
Alpinia Rhizome	China	52	5.2
Alpinia katsumadai Seed	Vietnam	52	5.2
Astragalus Root	Korea	52	5.2
Cinnamon Bark	Vietnam	52	5.2
Psoraleae Semen	China	106	10.6
Asiasarum Root and Rhizome	China	106	10.6
Evodia Fruit	China	106	10.6
Total amount		1000	100

Materials and Methods

Reagents. CellTiter 96 AQ_{ueous} One solution Cell Proliferation Assay (MTS) [3-(4,5-dimethylthiazol-2-yl)-5-(3-carboxymethoxy-phenyl)-2-(4-sulfophenyl)-2H-tetrazolium] was purchased from Promega (USA), propidium iodide (PI) was from Sigma (USA), and the pan caspase inhibitor, Z-VAD-fmk, was from R&D systems (USA). NE-PER Nuclear and Cytoplasmic Extraction Regents were purchased from Pierce (USA).

Plant materials. A5E consists of eleven Oriental medicinal herbs as shown in Table 1. The herbal ingredients were obtained from the Oriental Medical Hospital of Dongguk University (Korea) and kindly authenticated by Dr. Seonghyun Jeong (Department of Oriental Herbal Materials, Dongguk University).

Methods of extraction. The ethanol extract was prepared as follows. The dried and pulverized medicinal herbs were mixed, and a 1 kg batch was soaked with 40% ethanol (3 L). The ethanol extract was concentrated with a rotary evaporator, lyophilized, and reconstituted in distilled water for *in vitro* studies.

Gas chromatography-mass spectrometry analysis. GS-MS analysis of the herbal ethanol extract was performed on an Agilent 6890 GC/5973N mass-selective detector (Agilent Technologies, USA). A high-resolution capillary column, DM-5MS (30×250×0.25 cm), was used to separate the analytes. The oven temperature program was as follows: 50°C for 1 min, then 5°C/min until 280, and 280°C for 10 min. The front inlet temperature was maintained at 250°C. A split injection was used, with a split ratio of 5:1, and helium was used as the carrier gas at a flow rate of 1 mL/min; 1 μL of the sample was injected for analysis.

Antibodies. Antibodies against phospho-pRb, pRb, poly-(ADP-ribose) polymerase (PARP), caspase-3, caspase-8, caspase-9, p53, p-p53, phospho-Akt1/2/3 (Ser-473), Bcl-2, Bcl-xL, Bax, PCNA, and cytochrome C were purchased from Cell Signaling Technology (USA). α-Rabbit and α-mouse IgG horseradish peroxidase (HRP)-conjugated secondary antibodies were purchased from Millipore (USA). Antibodies against PI3K, Akt, p27, p21, NF-κB p65, actin, and GAPDH were purchased from Santa Cruz Biotechnology (Santa Cruz, USA). Antibodies specific to cyclin D1, cyclin E, and cyclin A were purchased from BD Bioscience (USA).

Cell culture. We obtained the human non small cell lung cancer cell lines NCI-H460 from the American type culture collection (ATCC; USA). Cells were cultured in Roswell Park Memorial Institution medium (Welgene Incorporation, Korea) supplemented with heat-inactivated 10 % (v/v) fetal bovine serum (Hyclone Laboratories, USA) and incubated under humidified conditions at 5% CO_2 and 37°C. Cells used in this study were subjected to no more than 20 cell passages.

Cell viability assays. The NCI-H460 cell line (0.7×10^4 cells) was seeded in 100 μL of medium in 96-well plates and incubated overnight. After 20 h of growth, the cells were treated with various concentration of A5E for 24 h. The cell viability was estimated using the MTS assay. Briefly, 100 μL of medium was removed, and 20 μL of MTS (2 mg/mL) and PMS mix solution (in RPMI medium) was added to each well and incubated for 1–2 h at 37°C. The absorbance was measured at 492 nm using an ELISA plate reader (Apollo LB 9110, Bertholo, Technologies GmbH, Germany).

Flow cytometry analysis after Annexin V and PI staining. Apoptotic cells were quantitated by flow cytometry using the Annexin V-fluorescein isothiocyanate (FITC) Apoptosis Detection Kit (BD Pharmingen, USA). NCI-H460 cells were seeded in 6-well plates at approximately 1.5×10^5 cells/well. A5E was added at various concentrations and incubated with the cells for 24 h. The cells were harvested, washed with phosphate buffered saline (PBS), and the cell pellets were then re-suspended in Annexin binding buffer. The cells were examined by flow cytometry using the FACSCalibur Flow Cytometry System and the Cell Quest Pro software (BD Bioscience, USA). FACS analysis scatter-graphs of Annexin V-FITC/PI staining showed four different cell types: double-negative stained cells (LL, lower left) were live cells, Annexin V positive/PI negative stained cells (LR, lower right) and Annexin V/PI double positive stained cells (UR, upper right) denoted early apoptosis and late apoptosis cells, and Annexin V negative/PI positive stained cells (UL, upper left) denoted necrosis or damage to cells.

Cell-cycle analysis by flow cytometry. The cell-cycle distribution was analyzed by PI staining and flow cytometry. NCI-H460 cells (1×10^4 cells/mL) were seeded in each well of a 6-well plate and exposed to various concentrations of A5E for 24 h. The cells were then harvested, fixed with ice-cold 70% ethanol, and stored at –20°C until analysis. After fixation, the cells were washed twice with cold PBS, centrifuged, and the supernatant was aspirated. The pellet was resuspended and stained in PBS containing 50 μg/mL PI and 100 μg/mL RNase A for 20 min in the dark. The DNA content was analyzed by flow cytometry on a FACSCalibur with the CellQuest software (BD Bioscience). The sub-G_1 population, hypodiploid (≤2N), fragmented DNA, is a important indicator of apopotosis.

Western-blot analysis. A5E-treated cells were collected by centrifugation at 72×*g*, 5 min, 4°C. The cells were then washed with ice-cold PBS and centrifuged at 1,890×*g*, 5 min, 4°C. The obtained cell pellets were resuspended in lysis buffer containing 50 mM Tris (pH 7.4), 1,500 mM sodium chloride, 1 mM ethylenediaminetetraacetic acid (EDTA), 1% NP-40, 0.25% sodium deoxycholate, 0.1% sodium dodecyl sulfate, and protease inhibitor cocktail. The cell lysates were incubated on ice for 2 h, and the lysates were clarified by centrifugation at 17,010×*g*, 30 min, 4°C. The protein concentration was determined using the Bradford assay (Bio-Rad, USA) with a UV/VIS Spectrophotometer (Biochrom, Bio-wave II, UK), and the concentration values were used to load equal amounts on protein gels. Cell lysates were separated on 10–2% sodium dodecyl sulfate polyacrylamide gel electrophoresis (SDS-PAGE) gels, and the protein bands were transferred to polyvinylidene difluoride membranes (Millipore). The membranes were blocked in Tris-buffered saline with Tween-20 [2.7 M NaCl, 53.65 mM KCl, 1 M Tris-HCl (pH 7.4), 0.1% Tween-20] containing 5% non-fat dried milk for 1 h at room temperature. The membranes were incubated for 2 h at room temperature with primary antibodies specific to each target protein. After washing three times, HRP-conjugated a-rabbit or a-mouse IgG secondary antibodies were incubated with the primary antibodies for 1 h at room temperature. After washing four times, blots were exposed by WEST-ZOL (plus) Western Blot Detection System (iNtRON Biotechnology, Korea).

Nuclear and cytoplasmic fractionation. A5E-treated cells were collected and fractionated with the NE-PER Nuclear and Cytoplasmic Extraction Reagents (Thermo Fisher Scientific, USA) according to the manufacturer's instructions. Briefly, the cells were collected by centrifugation at 1,980×g, 4°C, 5 min, washed with PBS, and recentrifuged. The cell pellet was suspended with buffer 1, vortexed, and incubated on ice for 10 min. Buffer 2 was then added and incubated with the cells for 1 min. The lysates were centrifuged at 16,000×*g*, 4°C, 5 min, and the supernatants were collected to afford the cytoplasmic extracts. Next, the insoluble pellets were resuspended in buffer 3, incubated on ice for 40 min, and centrifuged at 16,000×*g*, 4°C, 10 min. The supernatants were collected to obtain the nuclear extracts. The cytoplasmic and nuclear extracts were loaded on a SDS-PAGE gel.

Immunofluorescence microscopy. NCI-H460 cells were seeded on sterilized cover slides in 24-well plates (0.5×10^4 cells/well) and incubated overnight. The cells were then treated with various concentration of A5E. After 24 h, the cells on the cover slides were washed twice with serum-free medium, fixed, and permeabilized with ice-cold acetone for 10 min. The cover slide was washed three times with PBS and blocked with 0.1% bovine serum albumin (BSA) in PBS at room temperature for 30 min. Primary antibodies (NF-κB, Santa Cruz Biotechnology Cat. sc-8008) were diluted (1:100) in 0.1% BSA in PBS and attached to the cover slide overnight at 4°C. After washing three times with PBS, the cover slide was incubated with the secondary antibody (α-mouse FITC), diluted 1:400 with 0.1% BSA in PBS, for 1 h. The slide was washed three times with PBS, exposed to DAPI (1:1,000) for 10 s, and washed twice with PBS. The stained cells were visualized under an upright fluorescence microscope (Olympus, Japan).

Reverse-transcriptase polymerase chain reaction (RT-PCR) and real-time quantitative PCR (qPCR). The cells treated with A5E were collected and lysed using the easy-BLUE Total RNA Extraction Kit (iNtRON Biotechnology) according to manufacturer's instructions. Oligo(dT)-primed RNA (5 μg) was reverse transcribed with M-MuLV reverse transcriptase (New England Biolabs, USA). qPCR was performed with a relative quantification protocol using the Chromo 4 Real-Time PCR system and iQ™ SYBR® Green Supermix (Bio-Rad). All target genes were normalized to the expression of the housekeeping gene, GAPDH. Each sample was run with the following primer sets; FasL: 5'-GCA GCC CTT GAA TTA CCC AT-3' (forward), 5'-CAG AGG TTG GAC AGG GAA GAA-3' (reverse); FADD: 5'-ACC TCT TCT CCA TGC TG-3' (forward), 5'-CAC ACA GGT CTT CCC CA-3' (reverse); cIAP: 5'-CGT CTC CAA TGA CAA ACA GT-3' (forward), 5'-TAG TCC TCG ATG AAG AGA TG-3' (reverse) GAPDH: 5-GGC TGC TTT TAA CTC TGG TA-3' (forward), 5'-TGG AAG ATG GTG ATG GGA TT-3' (reverse). The expression changes are represented by the ratio of FasL, FADD and cIAP expression in NCI-H460 cells treated with A5E compared with the untreated control.

Analysis of mitochondrial transmembrane potential (MMP). The MMP ($\Delta\psi_m$) was measured by JC-1 staining and flow cytometry. JC-1 (5,5',6,6'-tetrachloro-1,1,3',3'-tetraethyl-benzimidazolyl-carbocyanine chloride) was purchased from Enzo (Farmingdale, USA). The NCI-H460 cells were seeded in 6-well plates (1×10^5 cells/well) and treated with various concentrations of A5E. After 24 h, the supernatants were transferred to 1.5-mL tubes, washed with warm PBS, and trypsinized. The cells were collected with supernatants in the tubes. JC-1 (5 μg/mL) was mixed until the precipitate disappeared. The cells were incubated in the dark for 10 min at 37°C. After 10 min, the cells were centrifuged at 300×*g*, 5 min, 4°C, washed twice with cold PBS, and resuspended with 200 μL of PBS. The solutions were sorted with the FACSCalibur instrument and analyzed using the CellQuest software (BD Bioscience). All steps were performed under reduced lighting.

Statistical analysis. Data are presented are the mean ± SEM of

Table 2 Volatile compounds identified in A5E

Compounds	Retention time (min)	Relative (%)
Dehydrocrepenynic acid methyl ester	19.027	1.12
2-Butanone, 4-phenyl- (CAS) Benzylacetone	21.443	3.44
Benzene, 1,2,3-trimethoxy-5-methyl- (CAS) Toluene	25.703	7.08
Benzene, 1,2-dimethoxy-4-(2-propenyl)- (CAS) Methyleugenol	25.778	3.89
Jasmolin II	25.979	2.68
2H-1-Benzopyran-2-one, 3,4-dihydro- (CAS) MELITOL	26.886	2.19
2H-Furo[2,3-h]-1-benzopyran-2-one (CAS) Angecilin	34.850	27.03
unknown	36.026	24.69
Methyldymron	38.482	0.76
9,12,15-Octadecatrienoic acid (Z,Z)-, trimethylsilyl ester	38.701	0.92
unknown	38.892	0.70
unknown	41.467	22.46
Ethyl linoleate	42.273	1.62
9-Octadecenoic acid (Z)-, methyl ester (CAS) Methyl oleate	42.378	1.42

the results from at least three independent experiments. The statistical significance was assessed with Student's *t*-test. $*p < 0.05$ or $**p < 0.005$ were considered statistically significant.

Results

The chemical content of A5E. A5E consists of eleven Oriental medicinal herbs. The composition is similar with A1E which we published previously (Bak et al., 2013). The difference between A1E and A5E is that A5E have Evodia fruit as a substitute for Dolichos seed. The eleven ingredients and their proportion (w/w) are listed in Table 1. We identified the potential medicinal components of the A5E extract using GC-MS (Fig. 1A). Compounds were identified by comparisons to library entries (library search hits >90% probable were viewed as likely hits). The major peak in the GC chromatogram was 2H-furo-[2,3-H]-1-benzopyran-2-one, also called angecin or angelicin. Table 2 lists the chemical components of the extract.

A5E inhibited NCI-H460 proliferation and induced apoptosis. At first, the effect of A5E on NCI-H460 was measured with the MTS assay. As shown in Fig. 1B, A5E showed dose-dependent cytotoxicity in a non-small cell lung cancer NCI-H460 cell line. The half maximal inhibitory concentration was 0.5 mg/mL. Therefore, we performed an additional study with less than the half maximal inhibitory concentration of A5E (0.125–0.5 mg/mL). We used the HaCaT normal keratinocyte cell line as control cell for indicating no harmful effects to normal cells. A5E showed no notable cytotoxicity in HaCaT (Fig. 1B). Thus, A5E inhibits lung cancer proliferation whearas does not affect normal cells. Next, we observed A5E-treated cells *via* phase contrast microscopy. A5E also induced cell morphological changes, including cytoplasmic condensation, cell shrinkage, detachment, and plasma membrane blebbing (Fig. 2A). To determine whether this cell death was due to apoptosis, we assessed Annexin V-FITC/PI staining on A5E treated NCI-H460 cells. As illustrated in Fig. 2B, apoptotic cells were increased in a dose-dependent manner in A5E-treated NCI-H460 cells.

A5E inhibits cell cycle progression and regulates cell cycle related factors. To clarify whether the anti-proliferative activity of A5E is due to cell cycle arrest, we performed PI staining of NCI-H460 cells and analyzed the stained cells by flow cytometry. The cell cycle peak was moved to sub-G_1, and the cell population at sub-G_1 increased with increasing concentrations of A5E (Figs. 3A and B). To ascertain whether A5E affects the cell cycle regulatory pathways, we investigated the protein level of cell cycle factors by Western Blotting. p53 which is a cell cycle regulator acting at the G_1/S phase, and its activated form phophorylated p53 (p-p53), were elevated by A5E. Moreover, p21 which is a p53 downstream effector, and p27 which is another cell cycle regulatory factor were also up-regulated, while cyclin D and cyclin A were down-regulated by A5E (Fig. 3C). pRb prevents replication of damaged DNA at the G_1 phase, and pRb is inactivated by phosphorylation. A5E inhibited the expression of p-pRb in NCI-H460 cells indicating that activation of pRb (Fig. 3C).

A5E regulated PI3K/Akt and NF-κB cellular survival pathway. It has been reported that p53 regulates the PI3K/Akt pathway (Astanehe et al., 2008); thus, we studied the PI3K/Akt pathway by Western Blotting. A5E-treated NCI-H460 cells showed that PI3K, Akt, and its activated form, phosphorylated Akt, were downregulated (Fig. 4A). Hence, Akt stimulated the transactivation subunit of NF-κB (Madrid et al., 2001). Next, we ascertained that A5E inhibited the NF-κB pathway. The total NF-κB level was decreased slightly, whereas the inhibitot of κB (IκB) level was not changed. Furthermore, IκB inactivated, phosphorylated form of IκB (p-IκB) was down-regulated (Fig. 4B). The nuclear fraction revealed that A5E also inhibited NF-κB translocalization to the nucleus (Figs. 4C and 4D). These results indicated that A5E regulates the PI3K/Akt and NF-κB cellular survival pathway.

A5E induced apoptosis through extrinsic and intrinsic pathways. Two major pathways in involved in Apoptosis: an extrinsic (death-receptor) pathway and an intrinsic (mitochondria-dependent) pathway. To explore the molecular mechanism of apoptosis induced by A5E, we studied about extrinsic and intrinsic

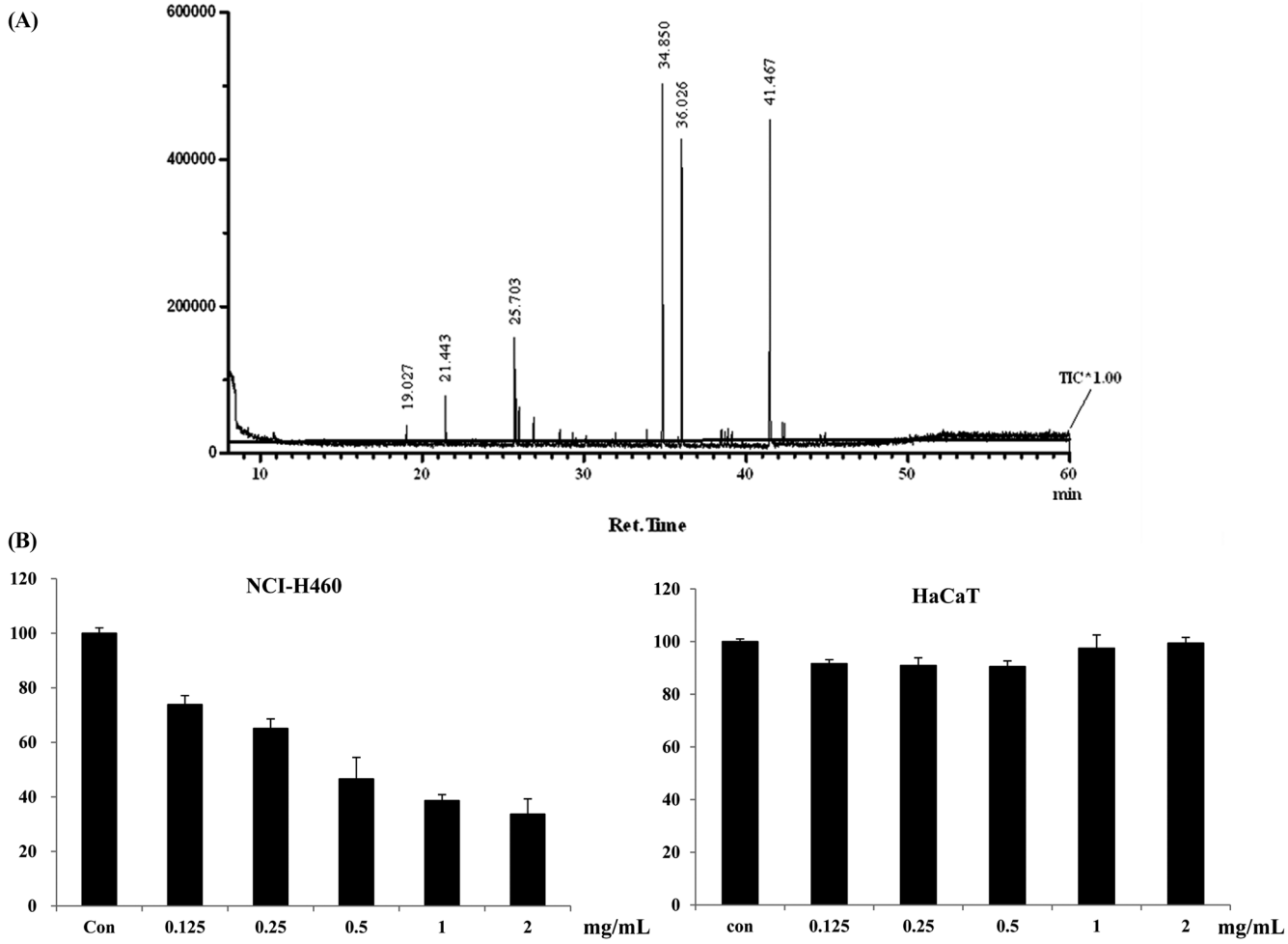

Fig. 1 Volatile components of the A5E ethanol extract identified by GC–MS (A), and anti proliferative effects of A5E on non small lung cancer and normal keratinocyte cell lines (B). The cell viability was measured with the MTS assay. A5E was incubated with non small cell lung cancer NCI-H460 cells, and normal keratinocyte HaCaT cells, with various concentrations (0.125–2 mg/mL) of A5E for 24 h. *p <0.05, compared to untreated control.

pathway. First, we investigated the death receptor pathway. FasL is a death receptor ligand, and FADD is an associated factor. A5E elevated the mRNA levels of FasL and FADD compared with the untreated H460 cells (Figs. 5A and B); Fas was not altered (data not shown). A5E can also suppress the mRNA level of cIAP in a dose-dependent manner (Fig. 5C). Second, we conducted JC-1 staining to measure the mitochondrial membrane potential collapse ($\Delta\psi_m$). As illustrated in Fig. 5D, A5E induced permeability transition pore (PTP) formation resulted in mitochondrial outer membrane permeabilization. To detect downstream factors of the two cell survival pathways, we performed Western Blotting. The death receptor pathway-related caspase-8 and the mitochondria-related caspase-9 were cleaved and turn into activated form. In addition, executioner caspase-3 and its target, PARP were cleaved by A5E (Fig. 5E). The above-described data revealed that A5E generated PTP and aided the release of apoptosis-related proteins. As PTP formed, cytochrome C was released to the cytosol, forming the apoptosome with Apaf and caspase-9. A5E also induced the release of cytochrome C (Fig. 5F). A5E affects the levels of the anti-apoptotic proteins Bcl-2 and Bcl-xl decreased, while the level of the pro-apoptotic protein Bax increased in a dose-dependent manner (Fig. 5F). To determine whether apoptosis is caspase-dependent or not, we pretreated the cells with a pan-caspase inhibitor, Z-VAD-FMK, before A5E treatment. The pan-caspase inhibitor blocked the cleavage of caspases 3, 8, 9 as well as PARP (Fig. 6A). The pan-caspase inhibitor recovered the cell cycle arrest induced by A5E (Figs. 6B and C). These results show that A5E triggered apoptosis *via* both the extrinsic and intrinsic cell survival pathways.

Discussion

Cancer is hyperproliferative disorder characterized by dysregulation of apoptosis, proliferation, invasion, and metastasis. Several studies have revealed that plant extracts have anticancer effects (Skandrani et al., 2010; Chen et al., 2011; Mou et al., 2011; Rezaei et al., 2012). Some scientists argue that pure compounds are less

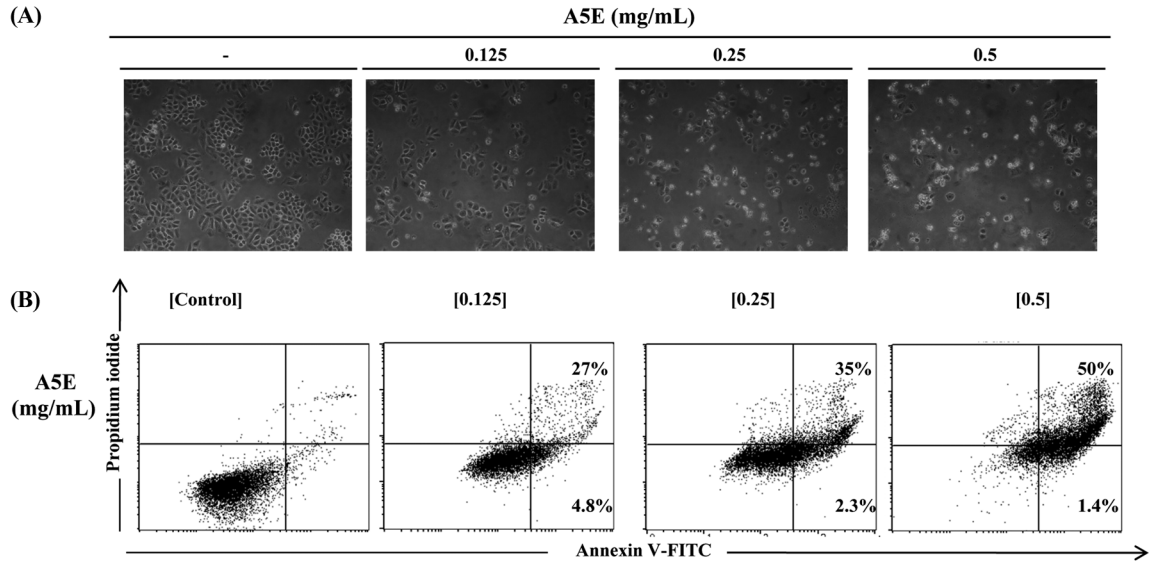

Fig. 2 Effect of A5E on cell morphology and apoptosis using NCI-H460 cells. NCI-H460 cells were treated with A5E (0.125–0.5 mg/mL) for 24 h. (A) Cell morphological changes were observed by phase contrast microscopy (100×). (B) The percentage of apoptotic cells was determined by FACS analysis and Annexin V-FITC/PI staining. Quadrant 1 contains late apoptotic cells (Annexin V and PI positive), and quadrant 4 contains early apoptotic cells (Annexin V positive and PI negative).

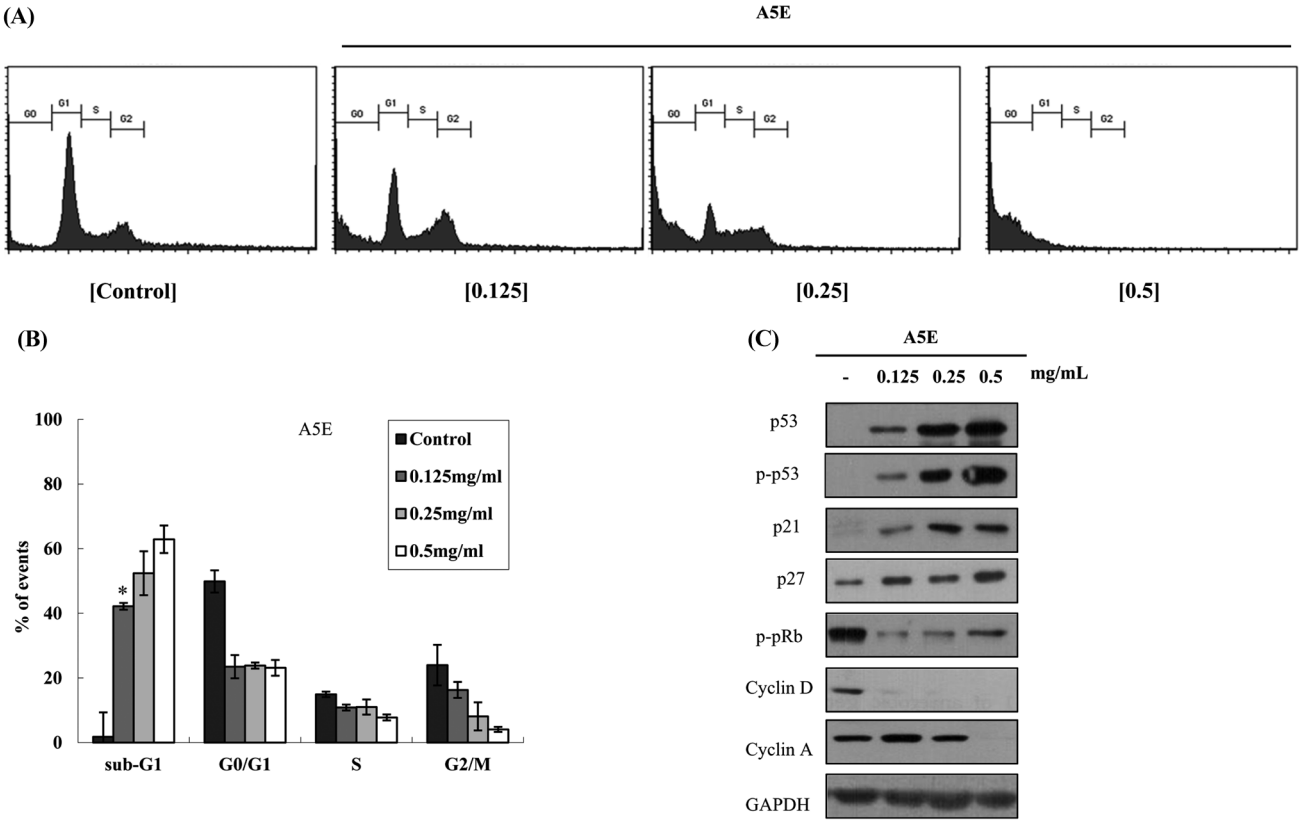

Fig. 3 Effect of A5E on cell cycle regulation using NCI-H460 cells. NCI-H460 cells treated with A5E were stained with PI and counted by flow cytometry. (A) Histogram of cell cycle distribution. (B) Bar graph of cell cycle distribution. Sub-G_1 cells increased by A5E treatment. A5E-treated NCI-H460 cells were lysed, and immunoblots were performed. (C) Immunoblots of cell cycle regulatory factors. GAPDH was used as internal control. *p <0.05, compared to untreated control.

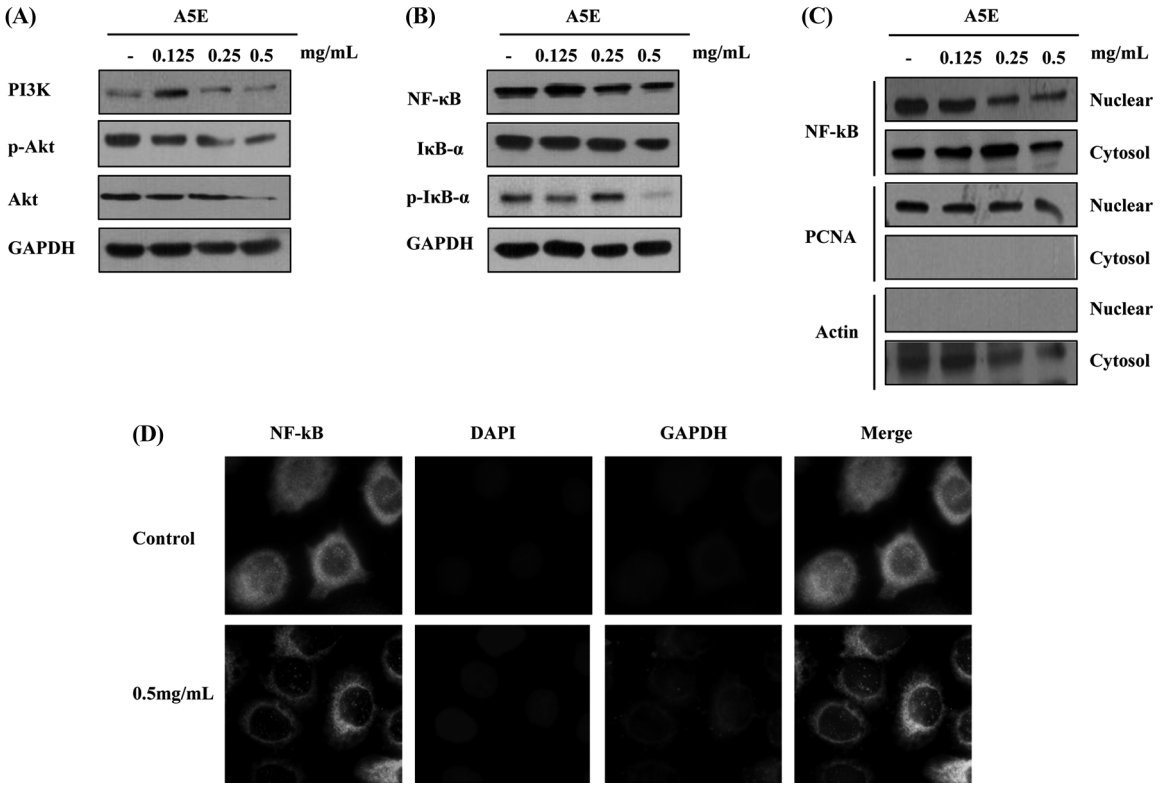

Fig. 4 Effects of A5E on the cell survival pathways using NCI-H460 cells. A5E-treated NCI-H460 cells were incubated for 24 h. Immunoblotting was performed. GAPDH was used as internal control. (A) PI3K/Akt pathway, (B) NF--κB pathway, (C) Fractionation of nuclear and cytosol contents for detection of NF-κB expression. (D) Immunofluorescence was performed. Green FITC was used for the target protein NF-κB, blue DAPI was used for nuclear staining, and red rhodamine was used for cytosol staining.

effective than extracts due to the loss of synergetic or additive effects in isolated material (Yi et al., 2005; Dai et al., 2007). Thus, we studied with A5E that traditional medical plant ethanol extract that includes ginseng and chaga. Our results revealed that angelicin is major component of A5E and Angelicin is a coumarin derivative with reported anticancer effects (Rahman et al., 2012). Therefore we hypothesized angelicin might contribute to the anticancer effects observed with A5E. In this reports, we investigated the anticancer effects of A5E with the NCI-H460 human non-small cell lung cancer cell line.

A5E treatment suppressed the growth of NCI-H460 cells determined by MTS assay. Judging from ANNEXIN V-PI staining data, growth suppression by A5E is due to apoptotic effects. Defects in cell cycle regulation lead to hyperproliferation of cells and the cancer development (Clarke and Allan, 2009). Apoptotic cell shows distinct characters such as cell morphological change and stagnant cell proliferation leading to death (Allen et al., 1997; Clarke and Allan, 2009). Each cell cycle is tightly regulated by cyclin, cyclin dependent kinase (cdk), and other factors (Satyanarayana and Kaldis, 2009). To verify A5E effects on cell cycle progression, we conducted cell cycle analysis and revealed that A5E inhibits cell cycle and induces cell to sub-G1 in NCI-H460. Overexpression of PI3K/Akt has been observed in many cancers (Falasca, 2010). Previous reports revealed that Akt inhibits p21 and p27 function through phosphorylation resulted in pRb phosphorylation (Brennan et al., 1997; Mitsuuchi et al., 2000). In addition, inhibition of cell survival *via* the PI3K/Akt pathway can induce apoptosis (Hussain et al., 2006; Gururajan et al., 2007). As expected, A5E also inhibited PI3K/Akt pathway indicating that A5E induce apoptosis through PI3K/Akt signal blockade. Hence, Akt has been shown to activate the transcription factor NF-κB (Ozes et al., 1999; Madrid et al., 2000) and our study revealed that A5E inhibit NF-κB translocation from cytosol to nucleus leading to block transcription of survival factor.

Apoptosis is generally divided into caspase-dependent and caspase-independent pathways (Denault and Boatright, 2004). The caspase-dependent pathway is divided into a death-receptor pathway and a mitochondria-dependent pathway. The caspase-independent pathway is an apoptosis-inducing factor (AIF)-dependent pathway (Mou et al., 2011). Anticancer drugs activate FasL, which binds Fas and triggers caspase-8 activation (Micheau et al., 1999). cIAP is an endogenous inhibitor of apoptosis, which inhibits the cleavage of caspase-8 and the truncation of Bid. Bax translocates into mitochondria and induces the opening of the mitochondrial voltage-dependent anion channel, VDAC (Wolter et al., 1997). Because mitochondria make ATP, mitochondria are crucial for survival. Mitochondria defects can be detected by a loss of MMP ($\Delta\psi_m$) (Chen et al., 2011) and A5E perturbed the

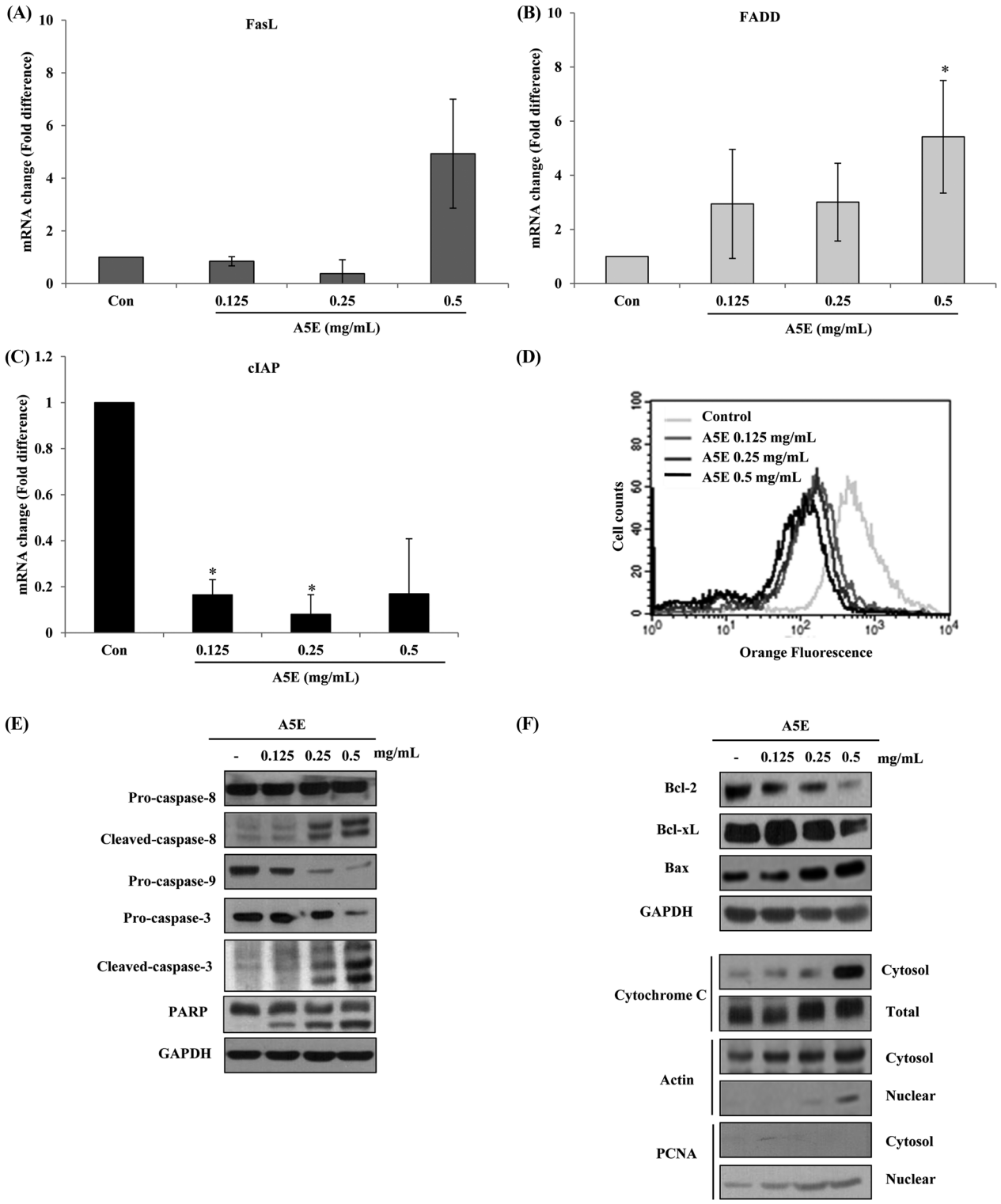

Fig. 5 Effects of A5E on apoptosis signaling using NCI-H460 cells. NCI-H460 cells were incubated with A5E for 24 h. RNA extraction and qRT-PCR were performed. The mRNA levels of (A) FasL and (B) FADD increased and (C) mRNA level of cIAP decreased. (D) JC-1 staining to detect the change in the MMP ($\Delta\psi_m$). GAPDH was used as internal control. The protein levels were determined by Western Blotting (E). Caspases 3, 8, and 9 as well as PARP were cleaved. (F) The levels of Bcl-2 and Bcl-xl decreased, while the level of Bax increased. Cytochrome C release was triggered by A5E. *p <0.05, compared to untreated control.

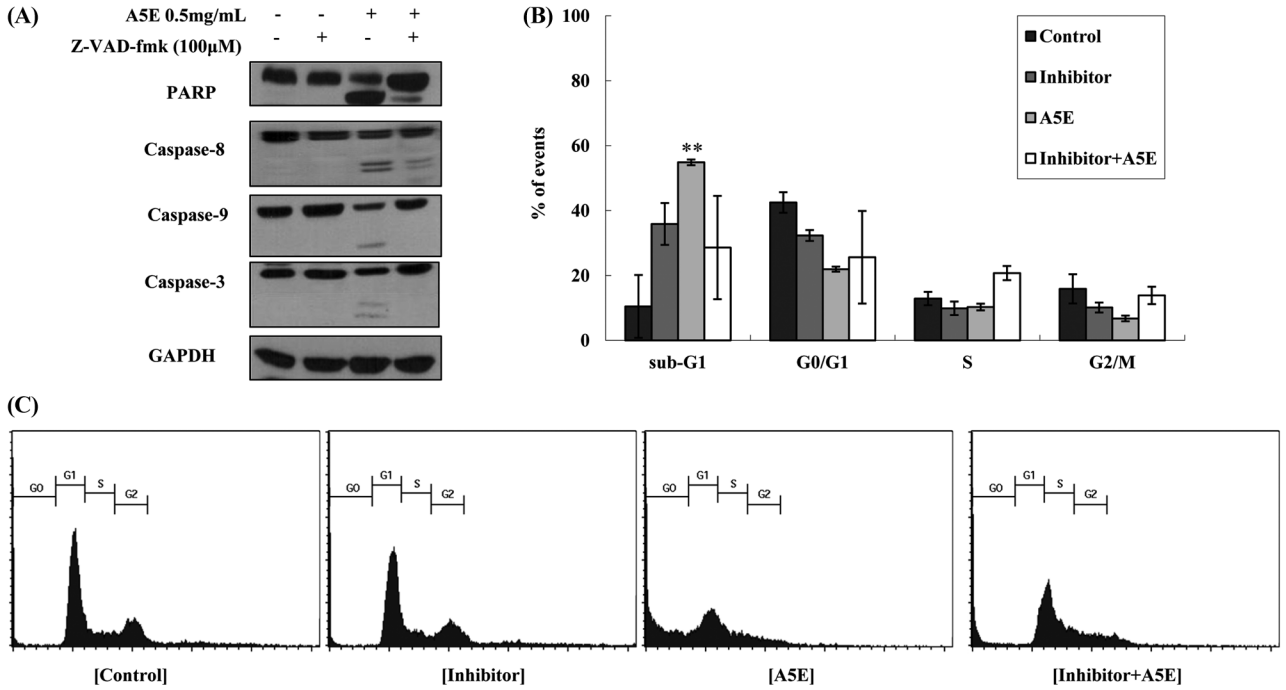

Fig. 6 Effects of A5E on the caspase-dependent pathway in NCI-H460 cells. NCI-H460 cells were treated with Z-VAD-fmk (100 μM) for 3 h before A5E treatment. (A) The pan-caspase inhibitor blocked caspase cleavage by A5E. (B, C) Pan-caspase inhibitor treatment recovered the cell cycle arrest by A5E. $^{**}p < 0.005$, compared to untreated control.

MMP and triggered the intrinsic pathway *via* the formation of caspase-9 and cytochrome C apoptosome. Bcl-2 and Bcl-xL have been identified as anti-apoptotic proteins that bind to the outer membrane of the mitochondria and prevent the release of cytochrome C. These proteins were inhibited by A5E. Bax is pro-apoptotic factor inducing cytochrome C release (Youle and Strasser, 2008) and A5E also increased Bax. Hence, A5E cleave executioner caspase-3 and its target protein PARP indicating that A5E provokes both extrinsic and intrinsic pathway. In conclusion, our results showed that A5E has a anti-proliferative, anti-cancer effect on non small cell lung cancer cells. Further studies are required to clarify the *in vivo* studies.

Acknowledgments This study was supported by a grant (B110053) from the Korean Health Technology R&D Project, Ministry of Health & Welfare, Republic of Korea. D.Y. was partially supported by a program (2012-0006686) of the National Research Foundation of Korea (NRF).

References

Allen RT, Hunter WJ, and Agrawal DK (1997) Morphological and biochemical characterization and analysis of apoptosis. *J Pharmacol Tox Met* **37**, 215–28.

Astanehe A, Arenillas D, Wasserman WW, Leung PC, Dunn SE, Davies BR et al. (2008) Mechanisms underlying p53 regulation of PIK3CA transcription in ovarian surface epithelium and in ovarian cancer. *J Cell Sci* **121**, 664–74.

Bak Y, Ham S, Baatartsogt O, Jung SH, Choi KD, Han TY et al. (2013) A1E inhibits proliferation and induces apoptosis in NCI-H460 lung cancer cells via extrinsic and intrinsic pathways. *Mol Bio Rep* **40,** 4507–19.

Brennan P, Babbage JW, Burgering BM, Groner B, Reif K, and Cantrell DA (1997) Phosphatidylinositol 3-kinase couples the interleukin-2 receptor to the cell cycle regulator E2F. *Immunity* **7**, 679–89.

Calviello G, Di Nicuolo F, Piccioni E, Marcocci ME, Serini S, Maggiano N et al. (2003) gamma-Tocopheryl quinone induces apoptosis in cancer cells via caspase-9 activation and cytochrome c release. *Carcinogenesis* **24**, 427–33.

Chen X, Pei L, Zhong Z, Guo J, Zhang Q, and Wang Y (2011) Anti-tumor potential of ethanol extract of Curcuma phaeocaulis Valeton against breast cancer cells. *Phytomedicine* **18**, 1238–43.

Chung MJ, Chung CK, Jeong Y, and Ham SS (2010) Anticancer activity of subfractions containing pure compounds of Chaga mushroom (Inonotus obliquus) extract in human cancer cells and in Balbc/c mice bearing Sarcoma-180 cells. *Nutr Res Pract* **4**, 177–82.

Clarke PR and Allan LA (2009) Cell-cycle control in the face of damage--a matter of life or death. *Trends Cell Biol* **19**, 89–98.

Dai J, Patel JD, and Mumper RJ (2007) Characterization of blackberry extract and its antiproliferative and anti-inflammatory properties. *J Med Food* **10**, 258–65.

Denault JB and Boatright K. (2004) Apoptosis in Biochemistry and Structural Biology. 3-8 February 2004, Keystone, CO, USA. *IDrugs* **7**, 315–7.

Falasca M (2010) PI3K/Akt signalling pathway specific inhibitors: a novel strategy to sensitize cancer cells to anti-cancer drugs. *Curr Pharm Design* **16**, 1410–6.

Fischer U, Janicke RU, and Schulze-Osthoff K (2003) Many cuts to ruin: a comprehensive update of caspase substrates. *Cell Death Differ* **10**, 76–100.

Gururajan M, Dasu T, Shahidain S, Jennings CD, Robertson DA, Rangnekar VM et al. (2007) Spleen tyrosine kinase (Syk), a novel target of curcumin, is required for B lymphoma growth. *J Immunol* **178**, 111–21.

Hsu HF, Houng JY, Kuo CF, Tsao N, and Wu YC (2008) Glossogin, a novel phenylpropanoid from Glossogyne tenuifolia, induced apoptosis in A549 lung cancer cells. *Food Chem Toxicol* **46**, 3785–91.

Hussain AR, Al-Rasheed M, Manogaran PS, Al-Hussein KA, Platanias LC, Al Kuraya K et al. (2006) Curcumin induces apoptosis via inhibition of

PI3'-kinase/AKT pathway in acute T cell leukemias. *Apoptosis* **11**, 245–54.

Jemal A, Siegel R, Xu J, and Ward E (2010) Cancer statistics, 2010. *CA Cancer J Clin* **60**, 277–300.

Kang TH, Bang JY, Kim MH, Kang IC, Kim HM, and Jeong HJ (2011) Atractylenolide III, a sesquiterpenoid, induces apoptosis in human lung carcinoma A549 cells via mitochondria-mediated death pathway. *Food Chem Toxicol* **49**, 514–9.

Kim AD, Kang KA, Zhang R, Lim CM, Kim HS, Kim DH et al. (2010) Ginseng saponin metabolite induces apoptosis in MCF-7 breast cancer cells through the modulation of AMP-activated protein kinase. *Environ Toxicol and Phar* **30**, 134–40.

Li GL, Jiang W, Xia Q, Chen SH, Ge XR, Gui SQ et al. (2010) HPV E6 down-regulation and apoptosis induction of human cervical cancer cells by a novel lipid-soluble extract (PE) from Pinellia pedatisecta Schott *in vitro*. *J Ethnopharmacol* **132**, 56–64.

Li WY, Chan SW, Guo DJ, Chung MK, Leung TY, and Yu PH (2009) Water extract of Rheum officinale Baill. induces apoptosis in human lung adenocarcinoma A549 and human breast cancer MCF-7 cell lines. *J Ethnopharmacol* **124**, 251–6.

Madrid LV, Mayo MW, Reuther JY, and Baldwin AS, Jr. (2001) Akt stimulates the transactivation potential of the RelA/p65 Subunit of NF-kappaB through utilization of the Ikappa B kinase and activation of the mitogen-activated protein kinase p38. *J Biol Chem* **276**, 18934–40.

Madrid LV, Wang CY, Guttridge DC, Schottelius AJ, Baldwin AS, Jr., and Mayo MW (2000) Akt suppresses apoptosis by stimulating the transactivation potential of the RelA/p65 subunit of NF-kappaB. *Mol Cell Biol* **20**, 1626–38.

Massion PP and Carbone DP (2003) The molecular basis of lung cancer: molecular abnormalities and therapeutic implications. *Resp Res* **4**, 12–27.

Micheau O, Solary E, Hammann A, and Dimanche-Boitrel MT (1999) Fas ligand-independent, FADD-mediated activation of the Fas death pathway by anticancer drugs. *J Biol Chem* **274**, 7987–92.

Mitsuuchi Y, Johnson SW, Selvakumaran M, Williams SJ, Hamilton TC, and Testa JR (2000) The phosphatidylinositol 3-kinase/AKT signal transduction pathway plays a critical role in the expression of p21WAF1/CIP1/SDI1 induced by cisplatin and paclitaxel. *Cancer Res* **60**, 5390–4.

Mou H, Zheng Y, Zhao P, Bao H, Fang W, and Xu N (2011) Celastrol induces apoptosis in non-small-cell lung cancer A549 cells through activation of mitochondria- and Fas/FasL-mediated pathways. *Toxicol In Vitro* **25**, 1027–32.

Ozes ON, Mayo LD, Gustin JA, Pfeffer SR, Pfeffer LM, and Donner DB (1999) NF-kappaB activation by tumour necrosis factor requires the Akt serine-threonine kinase. *Nature* **401**, 82–5.

Rahman MA, Kim NH, Yang H, and Huh SO (2012) Angelicin induces apoptosis through intrinsic caspase-dependent pathway in human SH-SY5Y neuroblastoma cells. *Mol Cel Biochem* **369**, 95–104.

Rezaei PF, Fouladdel S, Hassani S, Yousefbeyk F, Ghaffari SM, Amin G et al. (2012) Induction of apoptosis and cell cycle arrest by pericarp polyphenol-rich extract of Baneh in human colon carcinoma HT29 cells. *Food Chem Toxicol* **50**, 1054–9.

Satyanarayana A and Kaldis P (2009) Mammalian cell-cycle regulation: several Cdks, numerous cyclins and diverse compensatory mechanisms. *Oncogene* **28**, 2925–39.

Skandrani I, Pinon A, Simon A, Ghedira K, and Chekir-Ghedira L (2010) Chloroform extract from Moricandia arvensis inhibits growth of B16-F0 melanoma cells and promotes differentiation in vitro. *Cell Proliferat* **43**, 471–9.

Thafeni MA, Sayed Y, and Motadi LR (2012) Euphorbia mauritanica and Kedrostis hirtella extracts can induce anti-proliferative activities in lung cancer cells. *Mol Biol Rep* **39**, 10785–94.

Thompson CB (1995) Apoptosis in the pathogenesis and treatment of disease. *Science* **267**, 1456–62.

Wang L, Zhou GB, Liu P, Song JH, Liang Y, Yan XJ et al. (2008) Dissection of mechanisms of Chinese medicinal formula Realgar-Indigo naturalis as an effective treatment for promyelocytic leukemia. *P Natl Acad Sci USA* **105**, 4826–31.

Wolter KG, Hsu YT, Smith CL, Nechushtan A, Xi XG, and Youle RJ (1997) Movement of Bax from the cytosol to mitochondria during apoptosis. *J Cell Biol* **139**, 1281–92.

Yi W, Fischer J, Krewer G, and Akoh CC (2005) Phenolic compounds from blueberries can inhibit colon cancer cell proliferation and induce apoptosis. *J Agr Food Chem* **53**, 7320–9.

Youle RJ and Strasser A (2008) The BCL-2 protein family: opposing activities that mediate cell death. *Nat Rev Mol Cell Bio* **9**, 47–59.